CrossMark

Aerosol-Climate Interactions During the Last Glacial Maximum

Samuel Albani[1] · Yves Balkanski[1] · Natalie Mahowald[2] · Gisela Winckler[3,4] · Valter Maggi[5] · Barbara Delmonte[5]

Abstract

Purpose of Review Natural archives are imprinted with signs of the past variability of some aerosol species in connection to major climate changes. In certain cases, it is possible to use these paleo-observations as a quantitative tool for benchmarking climate model simulations. Where are we on the path to use observations and models in connection to define an envelope on aerosol feedback onto climate?

Recent Findings On glacial-interglacial time scales, the major advances in our understanding refer to mineral dust, in terms of quantifying its global mass budget, as well as in estimating its direct impacts on the atmospheric radiation budget and indirect impacts on the oceanic carbon cycle.

Summary Even in the case of dust, major uncertainties persist. More detailed observational studies and model intercomparison experiments such as in the Paleoclimate Modelling Intercomparison Project phase 4 will be critical in advancing the field. The inclusion of new processes such as cloud feedbacks and studies focusing on other aerosol species are also envisaged.

Keywords Aerosol · Mineral Dust · Last Glacial Maximum · Iron Fertilization · Radiative Forcing

Introduction

Aerosols are a key component of the climate system; yet their impacts on climate are still characterized by a high degree of uncertainty, because of the variety in physical and chemical composition, the complexity of their interactions, and the large spatial and temporal variability of emissions and dispersion [1, 2]. The temporal variability in aerosol emissions is imprinted

✉ Samuel Albani
samuel.albani@lsce.ipsl.fr

1 Laboratoire des Sciences du Climat et de l'Environnement, LSCE/IPSL, CEA-CNRS-UVSQ, Gif sur Yvette Cedex, France

2 Department of Earth and Atmospheric Sciences, Cornell University, Ithaca, NY, USA

3 Lamont-Doherty Earth Observatory of Columbia University, Palisades, NY, USA

4 Department of Earth and Environmental Sciences, Columbia University, New York, NY, USA

5 Department of Environmental and Earth Sciences, University of Milano-Bicocca, Milan, Italy

in both instrumental and paleoclimate records across a variety of time scales, including glacial-interglacial [3].

Aerosols directly impact the atmosphere radiation budget by the reflection and absorption of solar and terrestrial radiation. Depending on their size and chemical composition, specific aerosol species cause a net positive (black carbon) or negative (sulfates) direct radiative forcing, while other aerosol species have more complex net effects in different contexts [4]. Aerosols also affect climate by acting as cloud condensation nuclei (CCN) and ice nuclei (IN), thus affecting cloud lifetime and albedo [5, 6]. Absorbing aerosols can also impact cloud formation by heating, which can reduce relative humidity hence the liquid water path and/or cloud cover (semi-direct effect) [7, 8]. Finally, aerosols affect heterogeneous chemistry in the atmospheric environment [9]. Aerosol deposition to the surface can also impact climate. Snow albedo can be diminished by the presence of dust and especially black carbon (BC) [10, 11]. Last but not least, aerosols contribute elements such as phosphorus and iron to the terrestrial and marine biosphere, that can alter different global biogeochemical cycles and in turn the global carbon budget and climate [12].

Wind stress on the surface is tightly linked to the emissions of the most abundant natural primary aerosols. Mineral (desert) dust originates by eolian erosion from arid and semi-arid areas with low vegetation cover [13, 14], whereas

inorganic sea salts (mostly NaCl) are emitted as sea sprays at the air-water interface within breaking waves via bubble bursting and by tearing of wave crests [15], along with organic components [16]. Seawater brine and frost flowers forming on the surface of sea ice are a potentially important source of fractionated sea salt species, as well as organic matter [17, 18]. Land vegetation is also an important source of primary aerosols, either as primary biological aerosol particles (PBAPs) such as viruses, bacteria, fungal spores, pollen, plant debris, and algae [19, 20] or in the form of black carbon and particulate organic matter emitted via biomass burning (vegetation fires) [21]. Volcanic eruptions also emit ash [22]. Secondary aerosols can form from gaseous precursors: wetland emissions of ammonia, biogenic emissions of volatile organic compounds (BVOC) from terrestrial vegetation and biomass burning [23], and sulfate compounds from volcanic eruptions (SO_2) and marine biota (dimethyl sulfide) [17]. Natural nitrate aerosols are formed from sources of NO_x such as biomass burning, biogenic soil emissions, lightning, and stratospheric injection [24].

There is sometimes confusion about aerosol naming conventions. Different categorizations are possible, depending on [1] source process [2] chemical characterization as an airborne species or [3] operational definition when measured from sediments for the paleoclimate record. Here, we choose to organize the discussion around the potential of accumulation and measurement in paleoclimate archives.

Changing climate conditions that affect winds, the hydrological cycle and vegetation will affect aerosol emissions [25]. This is of interest for future climate change, where non-fossil fuel aerosol emissions can change along with direct anthropogenic emissions [26, 27], and it is relevant for the attribution of changes in the framework of the Intergovernmental Panel on Climate Change (IPCC). This is also relevant for climate, because of aerosols' feedback on the climate system [2, 28], as well as for public health [29, 30]. Past climate changes will also have caused differences in aerosol emissions, as evidenced by natural archives [31]. In the context of climatic changes, simulations of the past climate constitute a test bed for global Earth System Models (ESM), including for aerosols such as dust [32].

Driven by changes in the amount and distribution of incoming solar radiation, and mediated by internal feedbacks in the climate system, the last 100,000 years long glacial period culminated ~21,000 years before present (21 ka BP) during the last glacial maximum (LGM). The LGM was characterized by a significant drop in temperatures of several degrees, more markedly at high latitudes, associated to a massive reduction in the concentration of greenhouse gases compared to pre-industrial values [33]. Extensive ice sheets covered North America and West Eurasia, and the sea level was 120 m below the present level, associated with a reorganization of atmospheric and oceanic circulation, the hydrological

cycle, and ecosystems [34]. As we describe later, there is ample evidence that natural aerosol emissions were profoundly impacted by such climatic changes, in particular by changes in vegetation, glacial erosion and sea ice cover, and winds. Therefore, the LGM is an ideal target to explore natural aerosols (and dust in particular) interactions with climate.

Climate archives such as ice cores, marine sediments, lakes, peat bogs, and soil and loess profiles (Table 1) contain most of the information available about past aerosols. To interpret a paleoclimate record, the aerosol (or proxy) deposition flux to the surface of the archive needs to be connected to atmospheric concentrations of aerosols, and we need to understand how much the record is representative of larger scale patterns on different temporal and spatial scales [57]. Prognostic aerosol models represent a good example of process-based modeling—the modeling of a variable as it could be retrieved from a climate proxy [58]; in order to (almost) directly compare models with observations, the variable of interest is deposition flux, which for a meaningful model should include both dry and wet deposition processes [59].

Most of the information we have is about desert dust; dust is insoluble and, while it undergoes aging, it can be conserved to some extent in several natural archives from close to the source areas (e.g., loess) to remote sinks into the ocean or polar ice sheets [60]. Ice cores also preserve information about sea salt, sulfur and nitrogen species deposited to the surface [33]. Ice core data on carbonaceous aerosols is more limited, although some complementary information can be gathered, in terms of paleofire proxies, from charcoal, which offers chances of constraining Earth system models [56]. However, ice cores are limited in spatial coverage.

Some observations (Table 1) refer to the aerosol directly (e.g., particle counter dust measurements) or semi-directly (e.g., ^{232}Th for dust), and may be also used as a quantitative constraint of the aerosol mass in the past; other observations provide information about a process or a combination of processes, in which case we have a paleoclimate proxy in a traditional sense (e.g., ammonia for fires). In yet other cases both perspectives hold, e.g., desert dust is both a tracer and an agent of climate change. Besides determining the physical, chemical, and optical properties of aerosols, their mineralogical and/or elemental composition (including the isotope composition) may provide very useful insights onto geographical provenance and genesis processes (Table 1), as exemplified by dust radiogenic isotopes [33, 59].

Uncertainties from present day estimates of aerosols will propagate into the understanding of paleoclimate; for instance, modeling uncertainties in the parameterizations of cloud nucleation or the prescribed intrinsic optical properties of dust; or uncertainties in relating air-snow transfer of tracers. On the other hand, information from paleoclimate archives can also help to clarify some of these issues, and indeed provide a test for those models aiming to predict future climate change.

Table 1 Summary of the information on past aerosol from natural archives, relevant for the last glacial maximum

Type of aerosol	Natural archive	Measured property	Derived property	Comments and example reference
Mineral dust	Ice cores	Insoluble dust number and volume concentration (Coulter counter, laser optical counters)	Dust mass accumulation rates (MAR) and associated particle size distributions	The most direct measurement of dust, in "minimally disturbed" analytical conditions [35–37]
		Non sea salt calcium	Dust MAR	Proxy for dust, with uncertainties related to variable dust composition [38]
		Radiogenic isotope composition (Nd, Sr, Pb, Hf); rare earth elements (REE); relative abundance of major elements; mineralogy; and magnetic properties	Provenance fingerprinting	Spatial variability and limited sampling in potential source areas can be a limiting factor [39–42]
		Dust extinction and/or scattering (optical methods)	Shape and size-resolved intrinsic optical properties	Only a couple of pilot studies [43]
	Marine sediments	Mass of residual sediment after selective removal of opal and carbonates (operationally defined fraction)	Dust MAR	Usually used in combination with age-model-derived mass accumulation rates; no focusing corrections [44]
		Geochemical lithogenic proxies (e.g., Al, Ti, ^{232}Th, ^{4}He) concentration in sediment	Dust MAR	Usually used in combination with age-model-derived mass accumulation rate or, in the case of ^{232}Th, a constant flux-based mass accumulation rate ^{230}Th-excess, ^{3}He), to correct for sediment focusing [45–47]
		Laser optical counters	Particle size distributions	Use of dispersants: size may not be fully representative of atmospheric deposition [48]
		Radiogenic isotope composition (Nd, Sr, Pb); REE; ^{4}He/Th	Provenance fingerprinting	Spatial variability and limited sampling in potential source areas can be a limiting factor [49]
	Loess deposits	Radiocarbon or luminescence dating of soil horizons	Dust MAR	Reliability highly dependent on geomorphological settings and dating protocols [50, 51]
		Laser optical counters	Particle size distributions	Use of dispersants: size may not be fully representative of atmospheric deposition [52]
		Radiogenic isotope composition (Nd, Sr, Pb); REE	Provenance fingerprinting	Spatial variability and limited sampling in potential source areas can be a limiting factor [52]
Sea salts	Ice cores	Major ions, e.g., Na$^+$	Sea salt from open water and sea ice	Uncertainty in disentangling the two sources and interpreting the signal [53]
Sulfur species	Ice cores	SO$_4^{2-}$ and MSA	Sulfates: biogenic activity, volcanoes, and sea salt; MSA: biogenic emissions	Preservation issues for MSA. Very limited data, difficulties in interpreting the signal [54]
Nitrogen species	Ice cores	NO$_3^-$ and NH$_4^+$	Nitrate aerosol from lightning, fires, and biogenic emissions	Contamination and preservation issues. Very limited data, difficulties in interpreting the signal [54]
Carbonaceous aerosols	Ice cores	Organic carbon, formate, levoglucosan NH$_4^+$	Biogenic emissions, fires	Contamination and preservation issues. Very limited data, difficulties in interpreting the signal [55]
	Lakes sediments, peats, and soil	Charcoal	Source location of paleofires, type of burning regime	Geographical limitations in identifying the sources. Uncertainties in linking fires to type and amount of aerosol species [56]

Next, we will review the information arising from natural archives, and the state of the art in explaining the variability in LGM aerosol and understanding their feedback on climate, by targeting key scientific questions that have sparked research for the last decades or that are prone to become hot topics in the near future.

Climate Impacts on Aerosol Emissions

In this section, we review the information from paleoclimate archives concerning the major natural aerosol species documented for the LGM. For each aerosol species, we provide a brief description of the specific characteristics and the potential issues concerning the preservation of the depositional signal and estimates of the mass accumulation rates; we also describe the picture emerging from the specific paleoclimate records, as well as possible causes for observed changes in aerosol load/deposition rates.

Mineral Dust

Mineral dust is entrained in the atmosphere by wind erosion of sparsely vegetated soils or loose surface sediments [61]. It is composed mostly of silicates, along with carbonates and metal oxides, in the clay and fine silts dimensional range [62]. Aggregates have been observed [62], but their features are poorly understood, documented in the observational record, and represented in models [63, 64]. Dust composition, shape, and size combine to determine the intrinsic optical properties (mass extinction efficiency, single scattering albedo, asymmetry factor), which determine dust interaction with radiation [43, 65]. Pure mineral dust can be considered almost insoluble. This feature makes it a stable tracer that can be preserved in different environmental matrices, therefore potentially allowing the reconstruction of paleodust records from several natural archives (Table 1), including ice cores [35, 36], marine sediments [47, 66], loess/paleosol sequences [50, 52].

Extracting a paleodust record requires (1) preservation of the deposition signal, (2) the possibility to establish a chronology and (3) the possibility to isolate the eolian fraction, either operationally or geochemically, from the environmental matrix and other terrigenous components. In addition, it is necessary to verify that (4) the sediment accumulation rate is representative of the deposition flux to the surface [59].

Paleodust archives worldwide show a generalized two- to fivefold increase in dust deposition in the LGM compared to the Holocene [60], more marked at high latitudes [66–68]. Reconstructions from polar ice cores consistently show an order of magnitude variability in dust deposition flux between different climate states [35, 53]. These extreme variations are particularly evident in the Greenland ice core records [53, 69]. The cold climate—high dust relation holds over several

glacial interglacial cycles, as well as for millennial scale variability within glacial climates and during the last deglaciation [35, 47, 70, 71].

Several hypotheses have been proposed to explain glacial interglacial changes in paleodust records. Increased aridity [72, 73] and gustiness [51, 74, 75] are widespread conditions that could have enhanced dust emissions during glacial climate, when a general reduction of the hydrological cycle could also reduce wet scavenging and increase dust lifetimes [76, 77]. Additional mechanisms active at a more regional level could cause a characteristic geographic signature in specific paleodust archives in different geographical settings [78]. Source erodibility could be enhanced by reduced vegetation cover, linked to regional drying [79], and possibly reduced plant fertilization by CO_2 [80], and especially by increased sediment availability through glacial processes [39, 81], which is a well-established source of LGM dust at least in the Southern Hemisphere [82, 83], possibly also in connection to the exposure of continental shelves by lowered sea levels [40]. From an atmospheric transport perspective, reorganization of the atmospheric circulation between mid and high latitudes [35, 84], shifts in the intertropical convergence zone [85], and changes in the monsoonal variability [48] all contributed to shape the regional patterns of dust deposition in the LGM. In general, the LGM saw an expansion of mid and high latitude dust sources.

Global data compilations [59, 60, 80, 82, 86–89] allow for a generalized and consistent view of the geographical variability of the dust cycle, as well as constraining models, by comparing deposition fluxes from the models and mass accumulation rates for the observations in the same size range [86]. Model simulations including changes in dust sources (Fig. 1a) can be used in climate change experiments. The LGM climate constitutes an excellent test for dust; a model's spatial continuum can support the interpretation of paleodust archives [57], and yield quantitative estimates of the mass budget of the global dust cycle (Fig. 1c). Currently, only a few models, with diverse mechanisms to account for changes in dust sources, and diverse levels of validation against modern and paleodust data, have tried to simulate the LGM dust cycle [77, 82, 86, 90–98]; model emissions (loading) range from ∼ 2400 to ∼ 16,100 Tg a^{-1} (23 and 71 Tg) for the LGM, and between ∼ 1100 and ∼ 7100 Tg a^{-1} (8 and 36 Tg) for the corresponding pre-industrial/current climate control cases, with a median increase by a factor 2.0 (1.9) in the LGM (Fig. 1b, d).

The large spread is attributable to differences in the representation of dust emissions and deposition mechanisms, including from the dust schemes themselves, as well as differences in boundary conditions (including vegetation), the consideration of different aerosol size ranges, and lastly whether or not glaciogenic sources of dust (derived from glacier erosion) [81] were included. Each of these aspects contributes to the variability. Examples from specific studies illustrate and
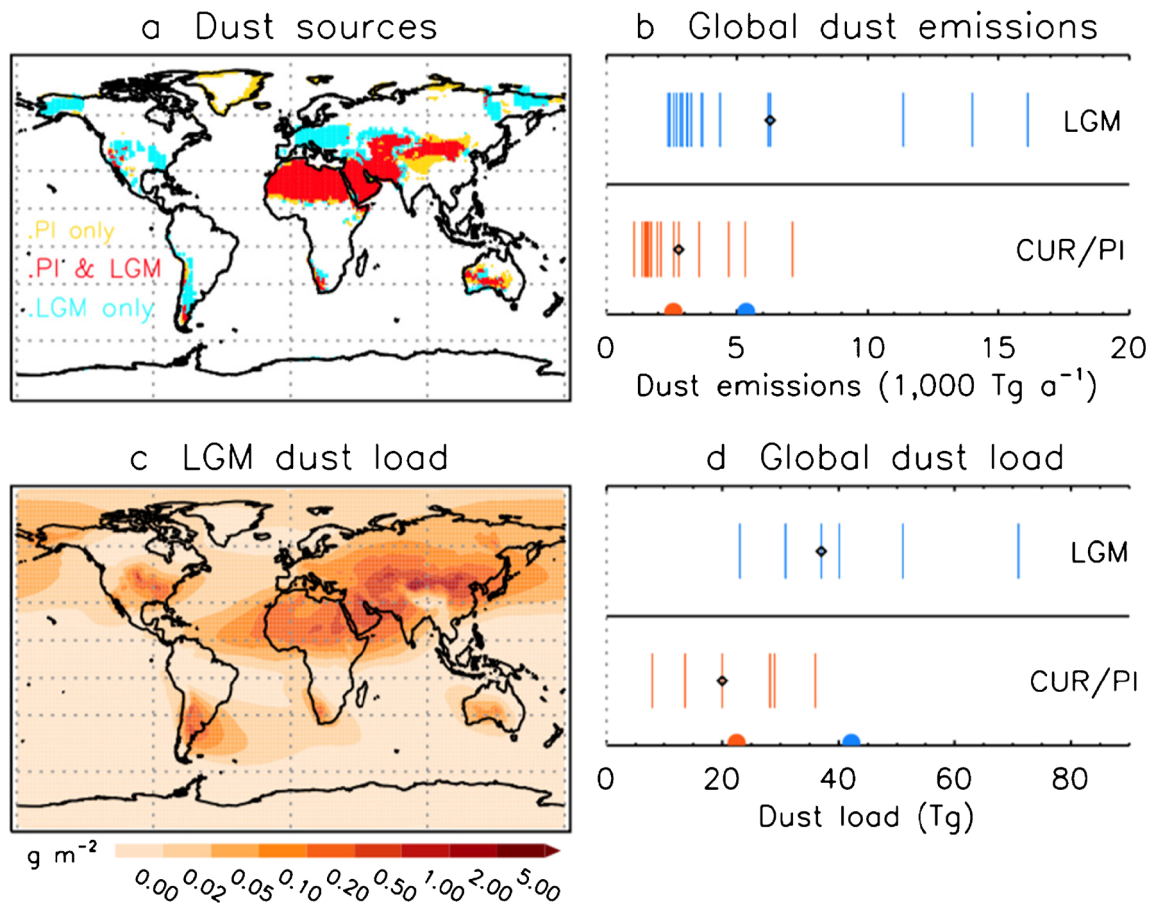
a Dust sources

b Global dust emissions

c LGM dust load

d Global dust load

Fig. 1 **a** Map of active sources for dust emissions in the LGM and pre-industrial (PI) conditions [90]. **b** Comparison of global mass budgets of dust emissions for LGM (upper panel, blue) and corresponding PI or CUR (PI/CUR) control (lower panel, red) for different climate model simulations [77, 82, 86, 90–97]. **c** Example map of dust load in the LGM [86]. **d** Global mass budget of dust load for LGM (upper panel,

blue) and PI/CUR control (lower panel, red) simulations [77, 86, 90, 91, 93–95]. The black diamonds in **b** and **d** highlight the simulations displayed in **a** and **c** [86, 90]. The semi-circles on the x-axis in **b** and **d** mark the average LGM (blue) and control (red) of the respective model ensembles. The vertical gray dotted lines mark the zero value on the x-axis

quantify the impacts of, e.g., allowing for source changes and using different emission schemes [80, 82, 95]. Future improvements anticipated to positively impact the representation of the dust cycle include the representation of physical climate boundary conditions, vegetation cover [91, 95], and glaciogenic sources [82, 86]. Dust sensitivity experiments planned for PMIP4 will provide an excellent opportunity to coherently compare LGM dust simulations for the first time [99]. Importantly, by exploiting the concept of process-based modeling, dust can be also viewed as a tracer and used as an indirect test to evaluate other components in the climate system, including vegetation, atmospheric circulation, and precipitation [58, 90].

Sea Salt

Here, we focus on the inorganic component of marine primary aerosols, i.e., sea salt from both open water [100] and sea ice [101–103]. Information about LGM sea salt deposition is derived from the interpretation of signals preserved in polar ice

cores (Table 1). This limits the spatial coverage of this kind of paleo-records compared to dust. Nonetheless, the location of polar ice cores in the proximity of high latitude oceans, where sea salt is the dominant aerosol species, offers an interesting chance for model validation.

Soluble Na^+ ions, stable in snow and ice, are considered the more robust indicators of sea salt depositional fluxes in Greenland and Antarctic ice core records, because crustal sodium contributions are considered negligible in relative terms, and be corrected for [54, 69]. Beside the dominant NaCl, other sea salts (Na_2SO_4, $CaSO_4$, $CaCO_3$) contribute to the ionic budgets in polar snow and ice; in particular, it has been noted that Na_2SO_4 is a species present in open water sea salts, but almost absent from sea ice salts originated from frost flowers, which can allow for disentangling the two sources based on considerations of ion balance and corrections based on standard sea water content [17, 104]. A few recent studies based on the sublimation of ice samples and the combination of microscopy and spectroscopic analyses helped the characterization in their solid state of soluble aerosols trapped in ice

cores, as well as variations in relative abundance in different climatic periods [105, 106].

The relative influence of sea salts in specific ice cores varies with the geographical location and proximity to the edges of the ice sheets, hence to the open water and sea ice sources [54]. In general terms, ice core records indicate that deposition rates of Na^+ in Antarctica increased by a factor of 3 to 5 during the LGM, compared to the Holocene [107–109]. Smaller increases, between 1.5 and 3 times the Holocene average if looking Na^+ accumulation rates or concentration in ice, were observed in Greenland [53, 110]. About whether concentrations in ice, rather than deposition fluxes, should be regarded as more representative of aerosol burden, some have argued that, because of changes in snow accumulation and aerosol deposition mechanisms, concentrations in ice are more informative than deposition fluxes in areas where wet deposition of aerosol dominates over dry deposition, and vice versa [57, 69].

Changes in sources (sea ice cover), emission strength and transport pathways (wind speed, cyclogenesis), and residence time (reduced wet scavenging) have all been invoked as possible candidates to explain glacial-interglacial variability in sea salt deposition to polar ice sheets [69, 111]. Because only ice cores are available to compare against for the LGM, open ocean sea salts emissions from the mid and low latitudes, which should be the most important for radiative forcing, cannot be validated in these comparisons.

Very few modeling studies attempted to simulate the LGM sea salt aerosols. Experiments considering only an open ocean source estimated LGM (current/pre-industrial control) emissions of ~ 5700 (~ 6000) Tg a^{-1} [112], ~ 3400 (~ 4000) Tg a^{-1} [93], and ~ 4100 (~ 4300) Tg a^{-1} [113], respectively. The general slight decrease observed in those studies, as well as in others focusing more on the comparison with specific ice core records [114, 115], was generally attributed to an increase sea ice cover, which reduces the source areas and increases the distance from source to sink. On the other hand, by also including a sea ice source, Yue and Liao found an increase of almost 200% in their LGM global emissions, reaching ~ 11,900 Tg a^{-1} [113]. In general, studies incorporating a sea ice source found a significant increase in emissions, improving the comparison with, but still underestimating, sea salt deposition fluxes from ice core records in terms of Na^+ deposition rates [93, 112, 113, 115] or modern atmospheric concentrations [116].

Sulfur and Nitrogen Species

The major sources of natural sulfur aerosol in polar ice are phytoplankton's emissions of dimethyl sulfide (DMS), which is oxidized into methane sulfonic acid (MSA) and H_2SO_4 in the atmospheric environment. These two species can be measured in ice core samples via ion chromatography [54]. SO_4^{2-}

anions are stable in snow and ice, and those produced from the DMS oxidation pathway are a major contributor to the total SO_4^{2-} budget, which also includes contributions from volcanic activity and sea salt. The fraction of non-sea salt sulfates can be artificially separated from the total SO_4^{2-} budget by subtracting the sea salt fraction, based on the standard $Na^+:SO_4^{2-}$ ratio in sea water; the presence of sea ice salts depleted in sulfates complicates this kind of exercise [54, 107], adding uncertainty to a quantitative separation of different sources of sulfate aerosol in polar ice. On the other hand, it was shown that MSA has preservation issues in present-day conditions [117], whereas the presence of larger amounts of dust in the LGM is thought to have stabilized its preservation by offering the potential for fixation of the MS^- anion onto particulate material [107].

Ice core data suggests no significant glacial-interglacial variations in non-sea salt sulfate deposition fluxes to Antarctica [107], in contrast to increase in MSA LGM fluxes [118, 119], which are nonetheless affected by preservation issues. In contrast, an increase of ~ 2 of non-sea salt sulfate deposition fluxes was observed in Greenland [53]. In general, substantial uncertainties still exist in reconstructing and understanding the LGM sulfur cycle. Modeling studies [120] and present day observations [121] may help shed some light on these issues.

A few records of NO_3^- and NH_4^+ from polar ice cores also exist [122], although some concern arises from potential contamination and/or proven preservation issues, especially for nitrates [123]. The few existing records indicate an increase in LGM nitrate deposition fluxes in both Greenland [53] and Antarctica [124]. Very little is known about nitrate deposition on polar snow, although the analysis of NO_3^- oxygen isotopes has emerged as a viable tool to make inferences about the potential sources [125]. On the other hand, NH_4^+ records indicate larger fluxes during interglacials [122, 126]. In general, there is so far too little information to make robust inferences about the magnitude and causes of variations in nitrogen aerosol species on these time scales.

Since most of the radiative forcing from these short-lived aerosols will come from the concentration in tropical and mid-latitude regions, which are not sampled by polar ice cores, there are limits to how much information we can obtain [1].

Carbonaceous Aerosols

Black carbon is also referred to as elemental carbon (char and soot). In terms of carbon mass budget, the BC concentration in present day continental atmosphere is about one order of magnitude lower than OC [127]. Natural OC aerosol is made up by primary organic aerosol (POA), and foremost by secondary organic aerosol (SOA) originated from volatile organic compounds (VOCs) [128]. BC is preferentially emitted during the flaming phase of a wildfire, whereas OC aerosols mostly

originate under smoldering conditions. The highly heterogeneous chemical composition of carbonaceous aerosols may give rise to confusion in the nomenclature used in the scientific literature, where different operational definitions appear [129].

There is limited direct information on BC and OC, from ice cores. Measurements of total/dissolved OC and speciation of carbonaceous aerosols have been carried out on surface snow or shallow firn cores and alpine ice cores [130, 131], but deeper paleoclimate records are very rare at best [132]. In particular, we are not aware of any record spanning the LGM that provides estimates of mass accumulation rates of carbonaceous aerosol species. A recent paper on variations in relative abundance of different types of fluorescent organic matter in West Antarctica indicates a stronger imprint of humic-like material during the Holocene compared to the LGM, interpreted as more expansive vegetation cover and increased production and degradation of complex organic matter in terrestrial environments [133].

On the other hand, chemical tracers of past fire activity have been sought and measured in snow and ice; while some of these species may not be direct measurements of the most important carbonaceous aerosol species, they have the potential to be related to the major aerosol emissions from paleofires, upon knowledge of a present day characterization of fire emissions and deposition of its proxies onto snow and ice [134]. In particular, ammonium, formate, and levoglucosan seem to be the most promising species so far applied to ice cores dating back several millennia, at least in Greenland [55]. Ammonia tends to be the dominant nitrogen species emitted during boreal forest fires that would leave a trace in Greenland ice, by deposition on the form of ammonium formate; levoglucosan is only produced by combustion of cellulose under smoldering conditions, although its chemical stability during transport is still uncertain [55].

Complementary to ice core tracers, charcoal sedimentary records from lakes, peat bogs, and soil profiles represent a proxy for paleofires. The global patterns of charcoal abundance and the relative variations at specific sites provide an indicator of the frequency, intensity, and extent of past fires [135]. The Global Charcoal Database collects and organizes such type of records [56, 135]. Synthesis from the Global Charcoal dataset indicates a consistent pattern of low fire activity in the LGM compared to the Holocene, with a few localized exceptions [56]. This is generally consistent with an overall reduction of land vegetation biomass acting as fuel for fires—at high latitudes, the reduced fire activity is also linked to the presence of the Laurentide and Fenno-Scandian ice sheets. Indication of reduced fire activity in Northern high latitudes in the LGM is also consistent with the only ice core proxy record from Greenland, i.e., the ammonium record from the North Greenland Ice core Project (NGRIP) [126].

In terms of other biogenic emissions from land vegetation, global simulations with an Earth system model estimated

isoprene emissions between ~250 and 850 TgC a^{-1} in the LGM depending on the assumptions on CO_2 sensitivity and temperature boundary conditions, and a decrease by 42–44% in total SOA burden compared to their pre-industrial control for their central case [136, 137].

In synthesis, the overall knowledge on LGM carbonaceous aerosol is very limited. By combining information from the source of fires with information of past vegetation [138] and linking with past and modern data from sinks like snow and ice [134], we might have the tools to evaluate and constrain models simulating past fire activity, hence potentially the emissions of carbonaceous aerosols from fire [136, 139, 140] and vegetation [137]. Additional information is therefore needed, to provide a constraint on the sinks of carbonaceous aerosols, from polar (and potentially some alpine) ice cores spanning the LGM.

Aerosol Feedbacks on Climate

We now review the available information concerning the evaluation and quantification of aerosol feedbacks on climate during the LGM, in terms of direct and indirect effects in the atmosphere [1], as well as in terms of indirect impacts on biogeochemical cycles [141].

Direct and Indirect Impacts on Atmospheric Radiation

Numerical models are the main tool for studying aerosol impacts on atmospheric radiation, because it is very difficult to establish a causal relation for co-variations of aerosols and other climate proxies from the paleoclimate records, perhaps with the exception of very large volcanic eruptions. This is not the case for dust impacts on ocean biogeochemistry, as discussed in the following section.

Because of the large variations and the evidence of the strong dust-climate coupling imprinted in the paleoclimate records, most of the modelers' attention was focused on dust. Still, of the few studies simulating the LGM dust cycle, only some also included climate feedbacks. The case of dust is very interesting and very challenging because of dust interaction with both solar short-wave (SW) and terrestrial long-wave (LW) radiation [86, 142], which, combined with particle size distributions and the underlying surface albedo [63, 143–145], can result in geographically distinct patterns characterized by either a positive or a negative direct radiative forcing (Fig. 2a). On top of that, the LGM is challenging in particular because of the uncertainties in constraining dust emissions and changes in surface albedo [77, 86, 95].

The existing model studies that include both SW and LW dust-radiation interactions estimate the net top of the atmosphere (TOA) direct radiative forcing (RF), either instantaneous or effective, in a range between − 0.02 and −
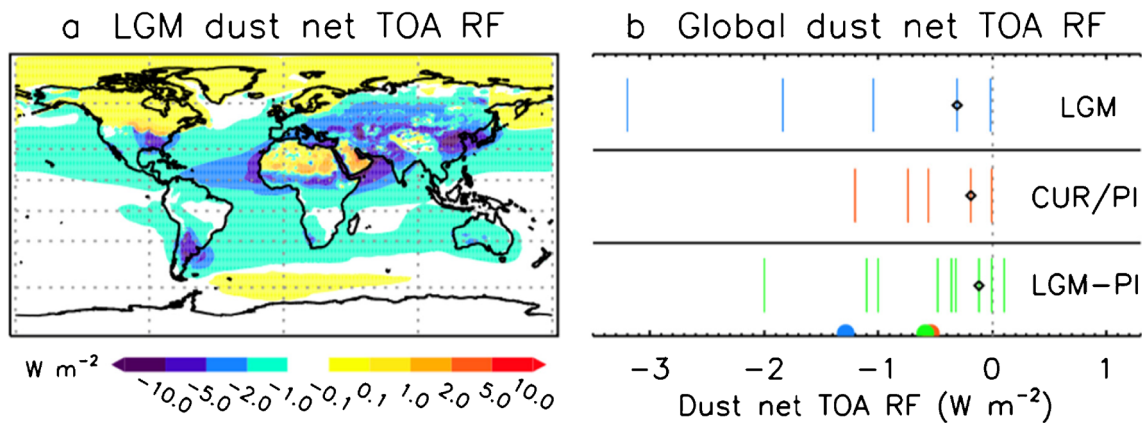
Fig. 2 **a** Example map of dust direct net (SW + LW) top of the atmosphere (TOA) instantaneous radiative forcing (RF) [86]. **b** Comparison of global estimates of dust direct net TOA RF from the literature, either in terms of instantaneous or effective RF, for LGM (upper panel, blue) and corresponding PI or CUR (PI/CUR) (middle panel, red) simulations [86, 90, 93, 95, 98, 146], and in terms of the LGM, control climate anomaly (bottom panel, green) [86, 90, 93–95, 98, 146]. The black diamonds in **b** highlight the simulation displayed in **a** [86]. The semi-circles on the x-axis in **b** mark the average LGM (blue), control (red), and anomaly (green) of the respective model ensembles. The vertical gray dotted line mark the zero value on the x-axis

3.2 W m^{-2} for the LGM, and between − 0.01 and − 1.2 W m^{-2} for the corresponding pre-industrial/current climate control cases; LGM-control climate anomalies range from − 2.0 to + 0.1 W m^{-2} (Fig. 2b). Note that here we considered only the control cases for the LGM simulations, not other studies focusing on pre-industrial or present day climate. For reference, for present day climate, IPCC AR5 estimated net TOA direct RF from dust in the range − 0.61 to + 0.10 W m^{-2} [1], whereas a recent study re-evaluating some of the former estimates in light of new constraints indicates a range from − 0.48 to + 0.20 W m^{-2} [147]. The large spread in RF estimates is probably linked to the spread in estimating dust loads (Fig. 1), as well as to differences in assumptions on dust particle size and optical properties. Note that because of the spatial variability in RF, even models showing relatively low global averages of net TOA RF may predict strong regional forcing (Fig. 2a).

Far fewer studies exist looking at other types of climate impacts. Dust impacts on snow albedo could have been an important mechanism preventing the development of an ice sheet in Northern Asia [148], and accelerating the retreat of the ice sheets during glacial terminations [149]. A recent study estimated indirect effects of dust onto clouds through ice nucleation processes in an idealized LGM simulation, indicating a significant increase in cloud cover, and a corresponding net TOA RF of − 1.1 W m^{-2} in the LGM, and − 0.5 W m^{-2} for their control climate [97]. One study estimated that the net TOA direct RF of sea salt from open water sources is − 0.92 W m^{-2} for their present day control simulation and − 0.96 W m^{-2} for the LGM, associated to a surface temperature anomaly of − 0.55 and − 0.5K, respectively; if the sea ice source is also included, the LGM impacts become larger, i.e., − 2.28 W m^{-2} and − 1.27K [113]. The global impacts associated with aerosols changes from the interglacial

reference period to the LGM are non-trivial, if compared to the major climate forcings characterizing the LGM climate, i.e., greenhouse gases (− 2.8 W m^{-2}) and ice sheets and sea level changes (− 3.0 W m^{-2}) [150].

In synthesis, we have a few model studies targeting the dust cycle in the LGM and its direct climate impacts. While this ensemble provides a first-order constraint of LGM dust direct feedbacks, a coherent analysis of their differences was never carried out. It is expected that dust experiments in PMIP4 will provide an opportunity to make progress in this sense [99]. Notably, the consistent use of the same model configuration for Climate Model Intercomparison Project phase 6, i.e., the CMIP6-PIMP4 experiments under different climate scenarios, including a pre-industrial control case, will also provide a common reference scenario for the LGM—as well as for present and future climate [151]—that was not consistently available for models shown in Figs. 1 and 2. The inclusion of additional processes such as ice nucleation in a few models could be an important step forward in for understanding and testing past climate variability.

Indirect Impacts on Biogeochemical Cycles

Mineral dust is thought to be the main aerosol species of relevance for global biogeochemical cycles during the LGM. Due to its mineralogical composition, mineral dust effectively acts as a windblown carrier for chemical elements, which can be transported and eventually deposited far from the dust source areas, impacting land and aquatic ecosystems. On land, in particular, there is evidence that on long time scales, dust-borne phosphorus can compensate the basin scale losses in the Amazon, maintaining the balance of this major nutrient [152, 153]. On the other hand, ocean ecosystems are most notably

impacted by inputs of silica and especially iron. The latter in particular is a micronutrient that can limit primary production at the ecosystem level [154]. This can be of great importance for high nutrient–low chlorophyll (HNLC) regions, where the primary production is relatively low despite the excess in major nutrients available for phytoplankton growth. The "iron hypothesis" postulates that enhanced inputs of dust-borne iron during glacial climate stimulated an increase in productivity in HNLC areas which in turn lead to increased carbon sequestration in the deep ocean drawing down atmospheric CO_2 concentrations [155]. This mechanism has been proposed to be a potentially relevant contributor to the ~ 80–100 ppmv observed decrease in atmospheric CO_2 concentration during the LGM, compared to pre-industrial levels [107, 155, 156]. Artificial iron fertilization experiments have clearly shown an increase in productivity in HNLC zones in response to iron inputs, but a quantification of the consequent deep carbon sequestration remains unclear [157].

Marine sediment records have the potential to provide critical information on this subject, provided that it is possible to derive a record of export production, and ideally nutrient utilization, that this can be related to iron inputs, and that the source of iron can be identified. Export production represent the fraction of organic matter that "escapes" remineralization (recycling in the photic zone) and reaches the sea floor; it can be estimated directly through the sedimentation rates of organic matter, often challenging because of preservation issues, or more often by a proxy such as mass accumulation rates of opal [158] and biogenic barium [159], or through the Pa/Th ratio [158, 160, 161]. In general, the consistency of multi-proxy reconstructions of export production and iron fluxes can be interpreted as an indicator of iron fertilization [157]. An additional constraint comes from the analysis of nitrogen isotopes in bulk sediment, foraminifera or diatoms, which is an indicator of nutrient utilization, and provides information on changes in the efficiency of major nutrient consumption [66, 162]. Finally, disentangling the role of different contributors to the iron budgets can clarify the actual mechanism of iron fertilization and allows for the quantification of the role of dust aerosol compared to other lithogenic inputs from the bottom, volcanic material, ice-rafted debris, or hydrothermal vents [163, 164].

The general view emerging from marine sediment cores [165], complemented by a number of recent studies (Fig. 3a), is that iron fertilization during glacial periods actually caused an enhancement of the efficiency of the ocean biological pump in specific regions [158, 183]. In particular, there is evidence that in the Southern Ocean, the most relevant HNLC area in terms of spatial scale and potential to influence the global carbon cycle, iron fertilization enhanced the efficiency of nutrient utilization [174]. In the subantarctic zone, this iron fertilization attributed to dust was also coupled to a net increase in export production, suggesting enhanced carbon sequestration in the deep ocean [167–169]. South of the polar front, a reduction of export production is observed, associated to diminished upwelling and increased stratification [165, 170, 183]. The other potentially relevant HNLC areas are the North and Equatorial Pacific (Fig. 3a). A study along the Line Islands in the central equatorial Pacific finds no evidence for iron fertilization by dust, nor increased export production or increased nutrient utilization, during the LGM [160]. A detailed investigation of three sediment cores, spanning the entire equatorial Pacific, showed that at each of the sites, biological productivity did not respond to increased dust
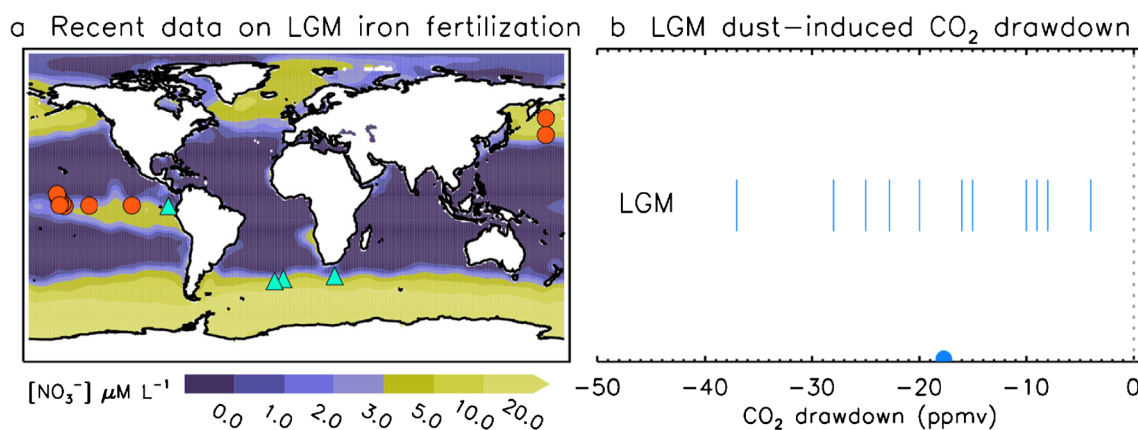

Fig. 3 a Map of present day high nutrient—low chlorophyll (HNLC) oceanic regions, indicated by patterns of nitrate concentrations in surface waters [166], along with the location of the most relevant recent core sites shading light on iron fertilization during the LGM [159, 160, 167–173]. The shape of the symbols indicate whether the observations suggest an increase (triangle) or not (circle) in export production in the LGM. The color of the symbols indicate whether observations suggest dust-driven iron fertilization in the LGM (green) or not (red). See also pre-existing global compilations of changes in ocean productivity in references (165, 174). b Model-based estimates of CO_2 drawdown induced by increased LGM dust deposition [175–182]. The semi-circle on the x-axis in b marks the average of the model ensemble. The vertical gray dotted line mark the zero value on the x-axis

deposition during glacial conditions, thus arguing against dust fertilization [159]. Both of these studies are inconsistent with prior work in the region [184]. In the subarctic North Pacific, the very limited studies seem to indicate that increases in export production mark the beginning of the deglaciation, rather than the LGM, and seem unrelated to dust activity or in general to iron inputs [68, 171, 172, 185].

Ocean biogeochemistry models can help quantify potential impacts of iron fertilization, if the inputs of dust [86, 90, 175] and other sources of iron are reasonably prescribed [186, 187]. A few studies with three-dimensional ocean biogeochemistry models of different complexity targeted the LGM, applying a variety of assumptions/strategies in terms of dust inputs, iron solubility, presence of iron-binding ligands, carbonate compensation, and even climate boundary conditions for their LGM dust experiments. In general, the models indicate that LGM dust-induced iron fertilization could be responsible for increased export production and for the associated drawdown of almost 20 ppmv of atmospheric CO_2, despite the large spread in estimates (Fig. 3b) and the difficulty in establishing a coherent comparison given the diversity on experimental designs [175–182]. Box model studies (not included in Fig. 3b) tend to indicate larger estimates of CO_2 drawdown [156, 188].

In synthesis, marine sediment core data generally agree on the occurrence of dust-borne iron fertilization as a mechanism that enhanced the efficiency of the biological pump and resulted in increased export production, at least in the subantarctic Southern Ocean [167, 189]. Ocean biogeochemistry models indicate a reduction of ~ 20 ppmv CO_2 during the LGM in response to iron fertilization [182]. The quantification of this effect and its impact on the global carbon cycle remain however highly uncertain, most notably because of uncertainties in the representation of key process in ocean biogeochemistry models [157], in the quantification of dust [90] and other potential sources of iron to HNLC areas in particular [186], and because of uncertainty in quantifying the bioavailable fraction of iron [190]. By considering combined uncertainties in dust deposition and iron solubility alone, a recent study estimated differences of a factor ~ 5 in soluble iron inputs to the ocean globally, and up to two orders of magnitude in the glacial Southern Ocean [90].

Additional paleodata from marine sediment cores, as well as future improvements in ocean biogeochemistry models, also driven by data from initiatives such as GEOTRACES [191] or process-based field campaigns, are needed to better quantify iron solubility [192–194] and indirect effects of dust on the ocean carbon cycle. Recent developments in explicitly representing mineralogy and aging in dust models [195–197] will provide enhanced tools to derive dust-borne iron inputs to the ocean, especially if also used for paleoclimate experiments and notably for the LGM [99].

Conclusions

The preservation of certain aerosol species in natural archives, along with other paleoclimate records, offers the opportunity to study the response of these aerosols' life cycle to changing climate conditions, and in some cases, it provides clues about aerosol feedbacks onto climate. Past climate variability since the last interglacial can be seen as an envelope of the potential natural aerosol variability, in terms of changing emissions as well as feedbacks onto climate. In particular, paleoclimate records from the LGM seem to indicate a decrease in aerosol emission from land vegetation, whereas emissions of dust and sea salt at mid and high latitudes were significantly enhanced.

For the LGM climate, mineral dust has received most of the attention, because of its preservation in several natural archives worldwide, the amplitude of its temporal variability, and its potential to impact climate directly and indirectly. While significant uncertainties still persist, dust seems likely an important contributor to the LGM climate forcing; enough knowledge has emerged to combine several models and observations, offering a unique opportunity to improve our understanding of the mechanisms controlling the global dust cycle, as well as its feedbacks onto climate. The LGM climate is also an ideal target to test the inclusion of new processes in models, such as iron fertilization of the oceans and ice nucleation in clouds.

The global budgets and causes of variability of other aerosol species are far less well constrained, although at least sea salt from open water and sea ice sources seems to be a near-future potential target, because of its potential direct and indirect effects on the atmospheric radiation balance, and the availability of some quantitative constraint on its variability from polar ice cores.

Ongoing and future work on constraining and modeling vegetation cover is a key aspect for the representation of past and future natural aerosol emissions, because of its tight link with dust emissions as well as for direct and post-fire aerosol and aerosol precursors' emissions.

In general, more observations are needed, in order to enhance the geographically resolved, quantitative constraints of aerosol mass budgets, and the understanding of specific processes. The coherent organization of such data into global databases is a key tool, allowing a holistic view of biogeochemical cycles, and providing a benchmark for global Earth system models aiming at predicting climate change.

In addition to LGM equilibrium climate conditions discussed in this manuscript, abrupt changes related to the deglaciation as well as glacial variability imprinted in natural archives [31, 198] offer a unique opportunity to improve our understanding of aerosols-climate interactions, provided that adequate observational databases can support modeling experiments [59].

Compliance with ethical standards

Conflict of Interest The authors declare no conflict of interest.

References

1. Boucher O, Randall D, Artaxo P, Bretherton C, Feingold G, Forster P. Clouds and aerosols. In: Stocker TF, et al., editors. Climate change 2013: the physical science basis contribution of working group I to the fifth assessment report of the intergovernmental panel on climate change. Cambridge and New York: Cambridge Univ. Press; 2013.

2. Carslaw KS, Boucher O, Spracklen DV, Mann GW, Rae JGL, Woodward S, et al. A review of natural aerosol interactions and feedbacks within the Earth system. Atmos Chem Phys. 2010;10(4):1701–37.

3. Augustin L, Barbante C, Barnes PRF, Marc Barnola J, Bigler M, Castellano E, et al. Eight glacial cycles from an Antarctic ice core. Nature. 2004;429(6992):623–8.

4. Myhre G, Samset BH, Schulz M, Balkanski Y, Bauer S, Berntsen TK, et al. Radiative forcing of the direct aerosol effect from AeroCom phase II simulations. Atmos Chem Phys. 2013;13(4): 1853–77.

5. Stevens B, Feingold G. Untangling aerosol effects on clouds and precipitation in a buffered system. Nature. 2009;461(7264):607–13.

6. Carslaw KS, Lee LA, Reddington CL, Pringle KJ, Rap A, Forster PM, et al. Large contribution of natural aerosols to uncertainty in indirect forcing. Nature. 2013;503(7474):67–71.

7. Johnson BT, Shine KP, Forster PM. The semi-direct aerosol effect: impact of absorbing aerosols on marine stratocumulus. Q J R Meteorol Soc. 2004;130(599):1407–22.

8. Storelvmo T. Aerosol effects on climate via mixed-phase and ice clouds. Annu Rev Earth Planet Sci. 2017;45(1):199–222.

9. Bauer SE, Balkanski Y, Schulz M, Hauglustaine DA, Dentener F. Global modeling of heterogeneous chemistry on mineral aerosol surfaces: influence on tropospheric ozone chemistry and comparison to observations. J Geophys Res Atmos. 2004;109(D2): D02304.

10. Painter TH, Flanner MG, Kaser G, Marzeion B, VanCuren RA, Abdalati W. End of the little ice age in the alps forced by industrial black carbon. Proc Natl Acad Sci. 2013;110(38):15216–21.

11. Di Mauro B, Fava F, Ferrero L, Garzonio R, Baccolo G, Delmonte B, et al. Mineral dust impact on snow radiative properties in the European Alps combining ground, UAV, and satellite observations. J Geophys Res Atmos. 2015;120(12):6080–97.

12. Mahowald NM. Aerosol indirect effect on biogeochemical cycles and climate. Science. 2011;334(6057):794–6.

13. Marticorena B, Bergametti G. Modeling the atmospheric dust cycle: 1. Design of a soil-derived dust emission scheme. J Geophys Res. 1995;100(D8):16415.

14. Prospero JM, Ginoux P, Torres O, Nicholson SE, Gill TE. Environmental characterization of global sources of atmospheric soil dust identified with the NIMBUS 7 Total Ozone Mapping Spectrometer (TOMS) absorbing aerosol product. Rev Geophys. 2002;40(1):2000RG000095.

15. de Leeuw G, Andreas EL, Anguelova MD, Fairall CW, Lewis ER, O'Dowd C, et al. Production flux of sea spray aerosol. Rev Geophys. 2011;49(2):2010RG000349.

16. Prather KA, Bertram TH, Grassian VH, Deane GB, Stokes MD, DeMott PJ, et al. Bringing the ocean into the laboratory to probe the chemical complexity of sea spray aerosol. Proc Natl Acad Sci. 2013;110(19):7550–5.

17. Rankin AM, Wolff EW. A year-long record of size-segregated aerosol composition at Halley, Antarctica. J Geophys Res Atmos. 2003;108(D24):2003JD003993.

18. Shaw PM, Russell LM, Jefferson A, Quinn PK. Arctic organic aerosol measurements show particles from mixed combustion in spring haze and from frost flowers in winter. Geophys Res Lett. 2010;37(10):L10803.

19. Després V, Huffman JA, Burrows SM, Hoose C, Safatov A, Buryak G, et al. Primary biological aerosol particles in the atmosphere: a review. Tellus Ser B Chem Phys Meteorol. 2012;64(1): 15598.

20. Fröhlich-Nowoisky J, Kampf CJ, Weber B, Huffman JA, Pöhlker C, Andreae MO, et al. Bioaerosols in the Earth system: climate, health, and ecosystem interactions. Atmos Res. 2016;182:346–76.

21. Andreae MO, Merlet P. Emission of trace gases and aerosols from biomass burning. Glob Biogeochem Cycles. 2001;15(4):955–66.

22. Robock A. Volcanic eruptions and climate. Rev Geophys. 2000;38(2):191–219.

23. Arneth A, Harrison SP, Zaehle S, Tsigaridis K, Menon S, Bartlein PJ, et al. Terrestrial biogeochemical feedbacks in the climate system. Nat Geosci. 2010;3(8):525–32.

24. Legrand MR, Kirchner S. Origins and variations of nitrate in south polar precipitation. J Geophys Res. 1990;95(D4):3493.

25. Tegen I, Schepanski K. Climate feedback on aerosol emission and atmospheric concentrations. Curr Clim Change Rep. 2018;4(1):1–10.

26. Ginoux P, Prospero JM, Gill TE, Hsu NC, Zhao M. Global-scale attribution of anthropogenic and natural dust sources and their emission rates based on MODIS Deep Blue aerosol products. Rev Geophys. 2012;50(3):2012RG000388.

27. Allen RJ, Landuyt W, Rumbold ST. An increase in aerosol burden and radiative effects in a warmer world. Nat Clim Chang. 2016;6(3):269–74.

28. Kok JF, Ward DS, Mahowald NM, Evan AT. Global and regional importance of the direct dust-climate feedback. Nat Commun. 2018;9(241):1–11.

29. Hansen J, Kharecha P, Sato M, Masson-Delmotte V, Ackerman F, Beerling DJ, et al. Assessing "dangerous climate change": required reduction of carbon emissions to protect young people, future generations and nature. PLoS One. 2013;8(12):e81648.

30. Fuzzi S, Baltensperger U, Carslaw K, Decesari S, Denier van der Gon H, Facchini MC, et al. Particulate matter, air quality and climate: lessons learned and future needs. Atmos Chem Phys. 2015;15(14):8217–99.

31. Steffensen JP, Andersen KK, Bigler M, Clausen HB, Dahl-Jensen D, Fischer H, et al. High-resolution Greenland ice core data show abrupt climate change happens in few years. Science. 2008;321(5889):680–4.

32. Kageyama M, Braconnot P, Harrison SP, Haywood AM, Jungclaus J, Otto-Bliesner BL, et al. The PMIP4 contribution to

CMIP6—part 1: overview and over-arching analysis plan. Geosci Model Dev. 2018;11:1033–105.

33. Petit JR, Jouzel J, Raynaud D, Barkov NI, Barnola J-M, Basile I, et al. Climate and atmospheric history of the past 420,000 years from the Vostok ice core, Antarctica. Nature. 1999;399:429–36.

34. Clark PU, Dyke AS, Shakun JD, Carlson AE, Clark J, Wohlfarth B, et al. The last glacial maximum. Science. 2009;325(5941):710–4.

35. Lambert F, Delmonte B, Petit JR, Bigler M, Kaufmann PR, Hutterli MA, et al. Dust-climate couplings over the past 800,000 years from the EPICA Dome C ice core. Nature. 2008;452(7187): 616–9.

36. Albani S, Delmonte B, Maggi V, Baroni C, Petit J-R, Stenni B, et al. Interpreting last glacial to Holocene dust changes at Talos Dome (East Antarctica): implications for atmospheric variations from regional to hemispheric scales. Clim Past. 2012;8(2):741–50.

37. Simonsen MF, Cremonesi L, Baccolo G, Bosch S, Delmonte B, Erhardt T, et al. Particle shape accounts for instrumental discrepancy in ice core dust size distributions. Clim Past Discuss. 2017 1–19.

38. Ruth U, Wagenbach D, Bigler M, Steffensen JP, Röthlisberger R, Miller H. High-resolution microparticle profiles at NorthGRIP, Greenland: case studies of the calcium–dust relationship. Ann Glaciol. 2002;35:237–42.

39. Delmonte B, Andersson PS, Schöberg H, Hansson M, Petit JR, Delmas R, et al. Geographic provenance of aeolian dust in East Antarctica during Pleistocene glaciations: preliminary results from Talos Dome and comparison with East Antarctic and new Andean ice core data. Quat Sci Rev. 2010;29(1–2):256–64.

40. Delmonte B, Paleari CI, Andò S, Garzanti E, Andersson PS, Petit JR, et al. Causes of dust size variability in central East Antarctica (Dome B): atmospheric transport from expanded South American sources during Marine Isotope Stage 2. Quat Sci Rev. 2017;168: 55–68.

41. Gabrielli P, Wegner A, Petit JR, Delmonte B, De Deckker P, Gaspari V, et al. A major glacial-interglacial change in aeolian dust composition inferred from Rare Earth Elements in Antarctic ice. Quat Sci Rev. 2010;29(1–2):265–73.

42. Lanci L, Delmonte B, Maggi V, Petit JR, Kent DV. Ice magnetization in the EPICA-Dome C ice core: implication for dust sources during glacial and interglacial periods. J Geophys Res. 2008;113(D14):2007JD009678.

43. Potenza MAC, Albani S, Delmonte B, Villa S, Sanvito T, Paroli B, et al. Shape and size constraints on dust optical properties from the Dome C ice core, Antarctica. Sci Rep. 2016;6(1):28162.

44. Hovan SA, Rea DK, Pisias NG. Late Pleistocene continental climate and oceanic variability recorded in Northwest Pacific sediments. Paleoceanography. 1991;6(3):349–70.

45. Middleton JL, Mukhopadhyay S, Langmuir CH, McManus JF, Huybers PJ. Millennial-scale variations in dustiness recorded in mid-Atlantic sediments from 0 to 70 ka. Earth Planet Sci Lett. 2018;482:12–22.

46. Serno S, Winckler G, Anderson RF, Hayes CT, McGee D, Machalett B, et al. Eolian dust input to the subarctic North Pacific. Earth Planet Sci Lett. 2014;387:252–63.

47. Winckler G, Anderson RF, Fleisher MQ, McGee D, Mahowald N. Covariant glacial-interglacial dust fluxes in the equatorial Pacific and Antarctica. Science. 2008;320(5872):93–6.

48. McGee D, deMenocal PB, Winckler G, Stuut JBW, Bradtmiller LI. The magnitude, timing and abruptness of changes in North African dust deposition over the last 20,000yr. Earth Planet Sci Lett. 2013;371–372:163–76.

49. Xie RC, Marcantonio F. Deglacial dust provenance changes in the eastern equatorial Pacific and implications for ITCZ movement. Earth Planet Sci Lett. 2012;317–318:386–95.

50. Moine O, Antoine P, Hatté C, Landais A, Mathieu J, Prud'homme C, et al. The impact of last glacial climate variability in west-

51. European loess revealed by radiocarbon dating of fossil earthworm granules. Proc Natl Acad Sci. 2017114(24):6209–14.

51. Muhs DR, Bettis EA III, Roberts HM, Harlan SS, Paces JB, Reynolds RL. Chronology and provenance of last-glacial (Peoria) loess in western Iowa and paleoclimatic implications. Quat Res. 2013;80(03):468–81.

52. Stevens T, Buylaert J-P, Lu H, Thiel C, Murray A, Frechen M, et al. Mass accumulation rate and monsoon records from Xifeng, Chinese Loess Plateau, based on a luminescence age model. J Quat Sci. 2016;31(4):391–405.

53. Mayewski PA, Meeker LD, Twickler MS, Whitlow S, Yang Q, Lyons WB, et al. Major features and forcing of high-latitude northern hemisphere atmospheric circulation using a 110,000-year-long glaciochemical series. J Geophys Res Oceans. 1997;102(C12): 26345–66.

54. Legrand M, Mayewski P. Glaciochemistry of polar ice cores: a review. Rev Geophys. 1997;35(3):219–43.

55. Legrand M, Preunkert S, Jourdain B, Guilhermet J, Faïn X, Alekhina I, et al. Water-soluble organic carbon in snow and ice deposited at Alpine, Greenland, and Antarctic sites: a critical review of available data and their atmospheric relevance. Clim Past. 2013;9(5):2195–211.

56. Marlon JR, Kelly R, Daniau A-L, Vannière B, Power MJ, Bartlein P, et al. Reconstructions of biomass burning from sediment-charcoal records to improve data–model comparisons. Biogeosciences. 2016;13(11):3225–44.

57. Mahowald NM, Albani S, Engelstaedter S, Winckler G, Goman M. Model insight into glacial–interglacial paleodust records. Quat Sci Rev. 2011;30(7–8):832–54.

58. Harrison SP, Bartlein PJ, Prentice IC. What have we learnt from palaeoclimate simulations? J Quat Sci. 2016;31(4):363–85.

59. Albani S, Mahowald NM, Winckler G, Anderson RF, Bradtmiller LI, Delmonte B, et al. Twelve thousand years of dust: the Holocene global dust cycle constrained by natural archives. Clim Past. 2015;11(6):869–903.

60. Kohfeld KE, Harrison SP. DIRTMAP: the geological record of dust. Earth-Sci Rev. 2001;54(1–3):81–114.

61. Shao Y, Wyrwoll K-H, Chappell A, Huang J, Lin Z, McTainsh GH, et al. Dust cycle: an emerging core theme in Earth system science. Aeolian Res. 2011;2(4):181–204.

62. Kandler K, Schütz L, Deutscher C, Ebert M, Hofmann H, Jäckel S, et al. Size distribution, mass concentration, chemical and mineralogical composition and derived optical parameters of the boundary layer aerosol at Tinfou, Morocco, during SAMUM 2006. Tellus Ser B Chem Phys Meteorol. 2009;61(1):32–50.

63. Mahowald NM, Albani S, Kok JF, Engelstaeder S, Scanza R, Ward DS, et al. The size distribution of desert dust aerosols and its impact on the Earth system. Aeolian Res. 2014;15:53–71.

64. Perlwitz JP, Pérez García-Pando C, Miller RL. Predicting the mineral composition of dust aerosols—part 1: representing key processes. Atmos Chem Phys. 2015;15(20):11593–627.

65. Formenti P, Schütz L, Balkanski Y, Desboeufs K, Ebert M, Kandler K, et al. Recent progress in understanding physical and chemical properties of African and Asian mineral dust. Atmos Chem Phys. 2011;11(16):8231–56.

66. Martínez García A, Rosell-Melé A, Geibert W, Gersonde R, Masqué P, Gaspari V, et al. Links between iron supply, marine productivity, sea surface temperature, and CO_2 over the last 1.1 Ma. Paleoceanography. 2009;24(1):PA1207.

67. Lamy F, Gersonde R, Winckler G, Esper O, Jaeschke A, Kuhn G, et al. Increased dust deposition in the Pacific Southern Ocean during glacial periods. Science. 2014;343(6169):403–7.

68. Serno S, Winckler G, Anderson RF, Maier E, Ren H, Gersonde R, et al. Comparing dust flux records from the subarctic North Pacific and Greenland: implications for atmospheric transport to

Greenland and for the application of dust as a chronostratigraphic tool. Paleoceanography. 2015;30(6):583–600.

69. Fischer H, Siggaard-Andersen M-L, Ruth U, Röthlisberger R, Wolff E. Glacial/interglacial changes in mineral dust and sea-salt records in polar ice cores: sources, transport, and deposition. Rev Geophys. 2007;45(1):2005RG000192.

70. Ruth U, Wagenbach D, Steffensen JP, Bigler M. Continuous record of microparticle concentration and size distribution in the central Greenland NGRIP ice core during the last glacial period. J Geophys Res Atmos. 2003;108(D3):4098.

71. Újvári G, Stevens T, Molnár M, Demény A, Lambert F, Varga G, et al. Coupled European and Greenland last glacial dust activity driven by North Atlantic climate. Proc Natl Acad Sci. 2017;114(50):E10632–8.

72. An Z, Kukla G, Porter SC, Xiao J. Late quaternary dust flow on the Chinese Loess Plateau. Catena. 1991;18(2):125–32.

73. Chylek P, Lesins G, Lohmann U. Enhancement of dust source area during past glacial periods due to changes of the Hadley circulation. J Geophys Res Atmos. 2001;106(D16):18477–85.

74. McGee D, Broecker WS, Winckler G. Gustiness: the driver of glacial dustiness? Quat Sci Rev. 2010;29(17–18):2340–50.

75. Roe G. On the interpretation of Chinese loess as a paleoclimate indicator. Quat Res. 2009;71(02):150–61.

76. Yung YL, Lee T, Wang C-H, Shieh Y-T. Dust: a diagnostic of the hydrologic cycle during the last glacial maximum. Science. 1996;271(5251):962–3.

77. Bauer E, Ganopolski A. Sensitivity simulations with direct shortwave radiative forcing by aeolian dust during glacial cycles. Clim Past. 2014;10(4):1333–48.

78. Albani S, Mahowald NM, Delmonte B, Maggi V, Winckler G. Comparing modeled and observed changes in mineral dust transport and deposition to Antarctica between the last glacial maximum and current climates. Clim Dyn. 2012;38(9–10):1731–55.

79. Lu H, Wang XY, Li LP. Aeolian sediment evidence that global cooling has driven late Cenozoic stepwise aridification in central Asia. In: Clift PD, Tada R, Zheng H, editors. Monsoon evolution and tectonics–climate linkage in Asia. London: Geological Society; 2010. p. 29–44.

80. Mahowald NM, Kohfeld K, Hansson M, Balkanski Y, Harrison SP, Prentice IC, et al. Dust sources and deposition during the last glacial maximum and current climate: a comparison of model results with paleodata from ice cores and marine sediments. J Geophys Res Atmos. 1999;104(D13):15895–916.

81. Bullard JE, Baddock M, Bradwell T, Crusius J, Darlington E, Gaiero D, et al. High-latitude dust in the Earth system. Rev Geophys. 2016;54(2):447–85.

82. Mahowald NM, Muhs DR, Levis S, Rasch PJ, Yoshioka M, Zender CS, et al. Change in atmospheric mineral aerosols in response to climate: last glacial period, preindustrial, modern, and doubled carbon dioxide climates. J Geophys Res Atmos. 2006;111(D10):D10202.

83. Sugden DE, McCulloch RD, Bory AJ-M, Hein AS. Influence of Patagonian glaciers on Antarctic dust deposition during the last glacial period. Nat Geosci. 2009;2(4):281–5.

84. Mayewski PA, Sneed SB, Birkel SD, Kurbatov AV, Maasch KA. Holocene warming marked by abrupt onset of longer summers and reduced storm frequency around Greenland. J Quat Sci. 2014;29(1):99–104.

85. Jacobel AW, McManus JF, Anderson RF, Winckler G. Climate-related response of dust flux to the central equatorial Pacific over the past 150 kyr. Earth Planet Sci Lett. 2017;457:160–72.

86. Albani S, Mahowald NM, Perry AT, Scanza RA, Zender CS, Heavens NG, et al. Improved dust representation in the community atmosphere model. J Adv Model Earth Syst. 2014;6(3):541–70.

87. Kienast SS, Winckler G, Lippold J, Albani S, Mahowald NM. Tracing dust input to the global ocean using thorium isotopes in

marine sediments: ThoroMap: ThoroMap. Glob Biogeochem Cycles. 2016;30(10):1526–41.

88. Maher BA, Prospero JM, Mackie D, Gaiero D, Hesse PP, Balkanski Y. Global connections between aeolian dust, climate and ocean biogeochemistry at the present day and at the last glacial maximum. Earth-Sci Rev. 2010;99(1–2):61–97.

89. Tegen I, Harrison SP, Kohfeld K, Prentice IC, Coe M, Heimann M. Impact of vegetation and preferential source areas on global dust aerosol: Results from a model study. J Geophys Res Atmos. 2002;107(D21):AAC 14–1–AAC 14–27.

90. Albani S, Mahowald NM, Murphy LN, Raiswell R, Moore JK, Anderson RF, et al. Paleodust variability since the last glacial maximum and implications for iron inputs to the ocean. Geophys Res Lett. 2016;43(8):3944–54.

91. Werner M, Tegen I, Harrison SP, Kohfeld KE, Prentice IC, Balkanski Y, et al. Seasonal and interannual variability of the mineral dust cycle under present and glacial climate conditions. J Geophys Res Atmos. 2002;107(D24):AAC 2–1.

92. Lunt DJ, Valdes PJ. Dust deposition and provenance at the last glacial maximum and present day. Geophys Res Lett. 2002;29(22):42-1—4.

93. Takemura T, Egashira M, Matsuzawa K, Ichijo H, O'ishi R, Abe-Ouchi A. A simulation of the global distribution and radiative forcing of soil dust aerosols at the last glacial maximum. Atmos Chem Phys. 2009;9(9):3061–73.

94. Yue X, Wang H, Liao H, Jiang D. Simulation of the direct radiative effect of mineral dust aerosol on the climate at the last glacial maximum. J Clim. 2011;24(3):843–58.

95. Hopcroft PO, Valdes PJ, Woodward S, Joshi MM. Last glacial maximum radiative forcing from mineral dust aerosols in an Earth system model. J Geophys Res Atmos. 2015;120(16):8186–205.

96. Sudarchikova N, Mikolajewicz U, Timmreck C, O'Donnell D, Schurgers G, Sein D, et al. Modelling of mineral dust for interglacial and glacial climate conditions with a focus on Antarctica. Clim Past. 2015;11(5):765–79.

97. Sagoo N, Storelvmo T. Testing the sensitivity of past climates to the indirect effects of dust: dust indirect effects in past climates. Geophys Res Lett. 2017;44(11):5807–17.

98. Claquin T, Roelandt C, Kohfeld K, Harrison S, Tegen I, Prentice I, et al. Radiative forcing of climate by ice-age atmospheric dust. Clim Dyn. 2003;20(2):193–202.

99. Kageyama M, Albani S, Braconnot P, Harrison SP, Hopcroft PO, Ivanovic RF, et al. The PMIP4 contribution to CMIP6—part 4: scientific objectives and experimental design of the PMIP4-CMIP6 last glacial maximum experiments and PMIP4 sensitivity experiments. Geosci Model Dev. 2017;10(11):4035–55.

100. O'Dowd CD, de Leeuw G. Marine aerosol production: a review of the current knowledge. Philos Trans R Soc A Math Phys Eng Sci. 2007;365(1856):1753–74.

101. Barber DG, Asplin MG, Papakyriakou TN, Miller L, Else BGT, Iacozza J, et al. Consequences of change and variability in sea ice on marine ecosystem and biogeochemical processes during the 2007–2008 Canadian International Polar Year program. Clim Chang. 2012;115(1):135–59.

102. Seguin AM, Norman A-L, Barrie L. Evidence of sea ice source in aerosol sulfate loading and size distribution in the Canadian High Arctic from isotopic analysis: frost flower influence on aerosols. J Geophys Res Atmos. 2014;119(2):1087–96.

103. Hara K, Matoba S, Hirabayashi M, Yamasaki T. Frost flowers and sea-salt aerosols over seasonal sea-ice areas in northwestern Greenland during winter–spring. Atmos Chem Phys. 2017;17(13):8577–98.

104. Udisti R, Dayan U, Becagli S, Busetto M, Frosini D, Legrand M, et al. Sea spray aerosol in central Antarctica. Present atmospheric

behaviour and implications for paleoclimatic reconstructions. Atmos Environ. 2012;52:109–20.

105. Oyabu I, Iizuka Y, Fischer H, Schüpbach S, Gfeller G, Svensson A, et al. Chemical compositions of solid particles present in the Greenland NEEM ice core over the last 110,000 years. J Geophys Res Atmos. 2015;120(18):9789–813.

106. Iizuka Y, Delmonte B, Oyabu I, Karlin T, Maggi V, Albani S, et al. Sulphate and chloride aerosols during Holocene and last glacial periods preserved in the Talos Dome Ice Core, a peripheral region of Antarctica. Tellus Ser B Chem Phys Meteorol. 2013;65(1): 20197.

107. Wolff EW, Fischer H, Fundel F, Ruth U, Twarloh B, Littot GC, et al. Southern Ocean sea-ice extent, productivity and iron flux over the past eight glacial cycles. Nature. 2006;440(7083):491–6.

108. Schüpbach S, Federer U, Kaufmann PR, Albani S, Barbante C, Stocker TF, et al. High-resolution mineral dust and sea ice proxy records from the Talos Dome ice core. Clim Past. 2013;9(6):2789–807.

109. Kaufmann P, Fundel F, Fischer H, Bigler M, Ruth U, Udisti R, et al. Ammonium and non-sea salt sulfate in the EPICA ice cores as indicator of biological activity in the Southern Ocean. Quat Sci Rev. 2010;29(1–2):313–23.

110. Spolaor A, Vallelonga P, Turetta C, Maffezzoli N, Cozzi G, Gabrieli J, et al. Canadian Arctic sea ice reconstructed from bromine in the Greenland NEEM ice core. Sci Rep. 2016;6(1):33925.

111. Petit JR, Delmonte B. A model for large glacial–interglacial climate-induced changes in dust and sea salt concentrations in deep ice cores (central Antarctica): palaeoclimatic implications and prospects for refining ice core chronologies. Tellus Ser B Chem Phys Meteorol. 2009;61(5):768–90.

112. Mahowald NM, Lamarque J-F, Tie XX, Wolff E. Sea-salt aerosol response to climate change: last glacial maximum, preindustrial, and doubled carbon dioxide climates. J Geophys Res. 2006;111(D5):2005JD006459.

113. Yue X, Liao H. Climatic responses to the shortwave and longwave direct radiative effects of sea salt aerosol in present day and the last glacial maximum. Clim Dyn. 2012;39(12):3019–40.

114. Genthon C. Simulations of desert dust and sea-salt aerosols in Antarctica with a general circulation model of the atmosphere. Tellus B. 1992;44(4):371–89.

115. Reader MC, McFarlane N. Sea-salt aerosol distribution during the last glacial maximum and its implications for mineral dust. J Geophys Res Atmos. 2003;108(D8):4253.

116. Levine JG, Yang X, Jones AE, Wolff EW. Sea salt as an ice core proxy for past sea ice extent: a process-based model study. J Geophys Res Atmos. 2014;119(9):5737–56.

117. Delmas RJ, Wagnon P, Goto-Azuma K, Kamiyama K, Watanabe O. Evidence for the loss of snow-deposited MSA to the interstitial gaseous phase in central Antarctic firn. Tellus B. 2003;55(1):71–9.

118. Legrand M, Feniet-Saigne C, Sattzman ES, Germain C, Barkov NI, Petrov VN. Ice-core record of oceanic emissions of dimethylsulphide during the last climate cycle. Nature. 1991;350(6314):144–6.

119. Watanabe O, Kamiyama K, Motoyama H, Fujii Y, Igarashi M, Furukawa T, et al. General tendencies of stable isotopes and major chemical constituents of the Dome Fuji deep ice core. Mem Natl Inst Polar Res. 2003;(57):1–24.

120. Castebrunet H, Genthon C, Martinerie P. Sulfur cycle at last glacial maximum: model results versus Antarctic ice core data. Geophys Res Lett. 2006;33(22):2006GL027681.

121. Legrand M, Preunkert S, Weller R, Zipf L, Elsässer C, Merchel S, et al. Year-round record of bulk and size-segregated aerosol composition in central Antarctica (Concordia site) part 2: biogenic sulfur (sulfate and methanesulfonate) aerosol. Atmos Chem Phys. 2017;17:14055–73.

122. Udisti R, Becagli S, Benassai S, De Angelis M, Hansson ME, Jouzel J, et al. Sensitivity of chemical species to climatic changes in the last 45 kyr as revealed by high-resolution Dome C (East Antarctica) ice-core analysis. Ann Glaciol. 2004;39:457–66.

123. Röthlisberger R, Hutterli MA, Wolff EW, Mulvaney R, Fischer H, Bigler M, et al. Nitrate in Greenland and Antarctic ice cores: a detailed description of post-depositional processes. Ann Glaciol. 2002;35:209–16.

124. Traversi R, Becagli S, Castellano E, Migliori A, Severi M, Udisti R. High-resolution fast ion chromatography (FIC) measurements of chloride, nitrate and sulphate along the EPICA Dome C ice core. Ann Glaciol. 2002;35:291–8.

125. Hastings MG, Sigman DM, Steig EJ. Glacial/interglacial changes in the isotopes of nitrate from the Greenland Ice Sheet Project 2 (GISP2) ice core. Glob Biogeochem Cycles. 2005;19(4):GB4024.

126. Fischer H, Schüpbach S, Gfeller G, Bigler M, Röthlisberger R, Erhardt T, et al. Millennial changes in North American wildfire and soil activity over the last glacial cycle. Nat Geosci. 2015;8(9): 723–7.

127. Pio CA, Legrand M, Oliveira T, Afonso J, Santos C, Caseiro A, et al. Climatology of aerosol composition (organic versus inorganic) at nonurban sites on a west-east transect across Europe. J Geophys Res. 2007;112(D23):D23S02.

128. Ruellan S, Cachier H, Gaudichet A, Masclet P, Lacaux J-P. Airborne aerosols over central Africa during the experiment for regional sources and sinks of oxidants (EXPRESSO). J Geophys Res Atmos. 1999;104(D23):30673–90.

129. Tsigaridis K, Daskalakis N, Kanakidou M, Adams PJ, Artaxo P, Bahadur R, et al. The AeroCom evaluation and intercomparison of organic aerosol in global models. Atmospheric. Chem Phys. 2014;14(19):10845–95.

130. McConnell JR, Edwards R, Kok GL, Flanner MG, Zender CS, Saltzman ES, et al. 20th-century industrial black carbon emissions altered Arctic climate forcing. Science. 2007;317(5843):1381–4.

131. Preunkert S, Legrand M. Towards a quasi-complete reconstruction of past atmospheric aerosol load and composition (organic and inorganic) over Europe since 1920 inferred from Alpine ice cores. Clim Past. 2013;9(4):1403–16.

132. Legrand M, McConnell J, Fischer H, Wolff EW, Preunkert S, Arienzo M, et al. Boreal fire records in northern hemisphere ice cores: a review. Clim Past. 2016;12(10):2033–59.

133. D'Andrilli J, Foreman CM, Sigl M, Priscu JC, McConnell JR. A 21 000-year record of fluorescent organic matter markers in the WAIS divide ice core. Clim Past. 2017;13(5):533–44.

134. Hawthorne D, Courtney Mustaphi CJ, Aleman JC, Blarquez O, Colombaroli D, Daniau A-L, et al. Global modern charcoal dataset (GMCD): a tool for exploring proxy-fire linkages and spatial patterns of biomass burning. Quat Int. 2017. In press

135. Power MJ, Marlon J, Ortiz N, Bartlein PJ, Harrison SP, Mayle FE, et al. Changes in fire regimes since the last glacial maximum: an assessment based on a global synthesis and analysis of charcoal data. Clim Dyn. 2008;30(7–8):887–907.

136. Murray LT, Mickley LJ, Kaplan JO, Sofen ED, Pfeiffer M, Alexander B. Factors controlling variability in the oxidative capacity of the troposphere since the last glacial maximum. Atmos Chem Phys. 2014;14(7):3589–622.

137. Achakulwisut P, Mickley LJ, Murray LT, Tai APK, Kaplan JO, Alexander B. Uncertainties in isoprene photochemistry and emissions: implications for the oxidative capacity of past and present atmospheres and for climate forcing agents. Atmos Chem Phys. 2015;15(14):7977–98.

138. Sánchez Goñi MF, Desprat S, Daniau A-L, Bassinot FC, Polanco-Martínez JM, Harrison SP, et al. The ACER pollen and charcoal database: a global resource to document vegetation and fire response to abrupt climate changes during the last glacial period. Earth Syst Sci Data. 2017;9(2):679–95.

139. Ward DS, Kloster S, Mahowald NM, Rogers BM, Randerson JT, Hess PG. The changing radiative forcing of fires: global model estimates for past, present and future. Atmos Chem Phys. 2012;12(22):10857–86.

140. Kloster S, Brücher T, Brovkin V, Wilkenskjeld S. Controls on fire activity over the Holocene. Clim Past. 2015;11(5):781–8.

141. Mahowald NM, Scanza R, Brahney J, Goodale CL, Hess PG, Moore JK, et al. Aerosol deposition impacts on land and ocean carbon cycles. Curr Clim Change Rep. 2017;3(1):16–31.

142. Perlwitz J, Tegen I, Miller RL. Interactive soil dust aerosol model in the GISS GCM: 1. Sensitivity of the soil dust cycle to radiative properties of soil dust aerosols. J Geophys Res Atmos. 2001;106(D16):18167–92.

143. Claquin T, Schulz M, Balkanski Y, Boucher O. Uncertainties in assessing radiative forcing by mineral dust. Tellus Ser B Chem Phys Meteorol. 1998;50(5):491–505.

144. Liao H, Seinfeld JH. Radiative forcing by mineral dust aerosols: sensitivity to key variables. J Geophys Res Atmos. 1998;103(D24): 31637–45.

145. Miller RL, Cakmur RV, Perlwitz J, Geogdzhayev IV, Ginoux P, Koch D, et al. Mineral dust aerosols in the NASA Goddard Institute for Space Sciences ModelE atmospheric general circulation model. J Geophys Res. 2006;111(D6):D06208.

146. Mahowald NM, Yoshioka M, Collins WD, Conley AJ, Fillmore DW, Coleman DB. Climate response and radiative forcing from mineral aerosols during the last glacial maximum, pre-industrial, current and doubled-carbon dioxide climates. Geophys Res Lett. 2006;33(20):L20705.

147. Kok JF, Ridley DA, Zhou Q, Miller RL, Zhao C, Heald CL, et al. Smaller desert dust cooling effect estimated from analysis of dust size and abundance. Nat Geosci. 2017;10(4):274–8.

148. Krinner G, Boucher O, Balkanski Y. Ice-free glacial northern Asia due to dust deposition on snow. Clim Dyn. 2006;27(6):613–25.

149. Ganopolski A, Calov R, Claussen M. Simulation of the last glacial cycle with a coupled climate ice-sheet model of intermediate complexity. Clim Past. 2010;6(2):229–44.

150. Braconnot P, Harrison SP, Kageyama M, Bartlein PJ, Masson-Delmotte V, Abe-Ouchi A, et al. Evaluation of climate models using palaeoclimatic data. Nat Clim Chang. 2012;2(6):417–24.

151. Carslaw KS, Gordon H, Hamilton DS, Johnson JS, Regayre LA, Yoshioka M, et al. Aerosols in the pre-industrial atmosphere. Curr Clim Change Rep. 2017;3(1):1–15.

152. Swap R, Garstang M, Greco S, Talbot R, Kallberg P. Saharan dust in the Amazon Basin. Tellus B. 1992;44(2):133–49.

153. Okin GS, Mahowald N, Chadwick OA, Artaxo P. Impact of desert dust on the biogeochemistry of phosphorus in terrestrial ecosystems. Glob Biogeochem Cycles. 2004;18(2):GB2005.

154. Jickells TD, An ZS, Andersen KK, Baker AR, Bergametti G, Brooks N, et al. Global iron connections between desert dust, ocean biogeochemistry, and climate. Science. 2005;308(5718): 67–71.

155. Martin JH, Gordon RM, Fitzwater SE. Iron in Antarctic waters. Nature. 1990;345(6271):156–8.

156. Archer DE, Johnson K. A model of the iron cycle in the ocean. Glob Biogeochem Cycles. 2000;14(1):269–79.

157. Tagliabue A, Bowie AR, Boyd PW, Buck KN, Johnson KS, Saito MA. The integral role of iron in ocean biogeochemistry. Nature. 2017;543(7643):51–9.

158. Kumar N, Anderson RF, Mortlock RA, Froelich PN, Kubik P, Dittrich-Hannen B, et al. Increased biological productivity and export production in the glacial Southern Ocean. Nature. 1995;378(6558):675–80.

159. Winckler G, Anderson RF, Jaccard SL, Marcantonio F. Ocean dynamics, not dust, have controlled equatorial Pacific productivity over the past 500,000 years. Proc Natl Acad Sci. 2016;113(22): 6119–24.

160. Costa KM, McManus JF, Anderson RF, Ren H, Sigman DM, Winckler G, et al. No iron fertilization in the equatorial Pacific Ocean during the last ice age. Nature. 2016;529(7587):519–22.

161. Hayes CT, Anderson RF, Fleisher MQ, Serno S, Winckler G, Gersonde R. Biogeography in 231Pa/230Th ratios and a balanced 231Pa budget for the Pacific Ocean. Earth Planet Sci Lett. 2014;391:307–18.

162. Altabet MA. Isotopic tracers of the marine nitrogen cycle: Present and past. In: Volkman JK, editor. Marine Organic Matter: Biomarkers, Isotopes and DNA. Berlin: Springer; 2006.

163. Abadie C, Lacan F, Radic A, Pradoux C, Poitrasson F. Iron isotopes reveal distinct dissolved iron sources and pathways in the intermediate versus deep Southern Ocean. Proc Natl Acad Sci. 2017;114(5):858–63.

164. Raiswell R, Hawkings JR, Benning LG, Baker AR, Death R, Albani S, et al. Potentially bioavailable iron delivery by iceberg-hosted sediments and atmospheric dust to the polar oceans. Biogeosciences. 2016;13(13):3887–900.

165. Kohfeld KE, Quéré CL, Harrison SP, Anderson RF. Role of marine biology in glacial-interglacial CO2 cycles. Science. 2005;308(5718):74–8.

166. Garcia HE, Locarnini RA, Boyer TP, Antonov JI, Baranova OK, Zweng MM, et al. Dissolved inorganic nutrients (phosphate, nitrate, silicate). In: Levitus S, editor. A. Mishonov, Technical Ed. NOAA Atlas NESDIS 7 6. (World Ocean Atlas 2013; vol. 4). 2013. 25 p

167. Martínez García A, Sigman DM, Ren H, Anderson RF, Straub M, Hodell DA, et al. Iron fertilization of the Subantarctic Ocean during the last ice age. Science. 2014;343(6177):1347–50.

168. Anderson RF, Barker S, Fleisher M, Gersonde R, Goldstein SL, Kuhn G, et al. Biological response to millennial variability of dust and nutrient supply in the Subantarctic South Atlantic Ocean. Philos Trans R Soc A Math Phys Eng Sci. 2014;372(2019): 20130054.

169. Ziegler M, Diz P, Hall IR, Zahn R. Millennial-scale changes in atmospheric CO2 levels linked to the Southern Ocean carbon isotope gradient and dust flux. Nat Geosci. 2013;6(6):457–61.

170. Jaccard SL, Hayes CT, Martinez-Garcia A, Hodell DA, Anderson RF, Sigman DM, et al. Two modes of change in Southern Ocean productivity over the past million years. Science. 2013;339(6126): 1419–23.

171. Lam PJ, Robinson LF, Blusztajn J, Li C, Cook MS, McManus JF, et al. Transient stratification as the cause of the North Pacific productivity spike during deglaciation. Nat Geosci. 2013;6(8): 622–6.

172. Ren H, Studer AS, Serno S, Sigman DM, Winckler G, Anderson RF, et al. Glacial-to-interglacial changes in nitrate supply and consumption in the subarctic North Pacific from microfossil-bound N isotopes at two trophic levels. Paleoceanography. 2015;30(9): 1217–32.

173. Loveley MR, Marcantonio F, Wisler MM, Hertzberg JE, Schmidt MW, Lyle M. Millennial-scale iron fertilization of the eastern equatorial Pacific over the past 100,000 years. Nat Geosci. 2017;10(10):760–4.

174. Kohfeld KE, Graham RM, de Boer AM, Sime LC, Wolff EW, Le Quéré C, et al. Southern hemisphere westerly wind changes during the last glacial maximum: paleo-data synthesis. Quat Sci Rev. 2013;68:76–95.

175. Lambert F, Tagliabue A, Shaffer G, Lamy F, Winckler G, Farias L, et al. Dust fluxes and iron fertilization in Holocene and last glacial maximum climates. Geophys Res Lett. 2015;42(14):6014–23.

176. Bopp L, Kohfeld KE, Le Quéré C, Aumont O. Dust impact on marine biota and atmospheric CO2 during glacial periods. Paleoceanography. 2003;18(2):1046.

177. Brovkin V, Ganopolski A, Archer D, Rahmstorf S. Lowering of glacial atmospheric CO2 in response to changes in oceanic

circulation and marine biogeochemistry. Paleoceanography. 2007;22(4):PA4202.

178. Parekh P, Follows MJ, Dutkiewicz S, Ito T. Physical and biological regulation of the soft tissue carbon pump. Paleoceanography. 2006;21(3):PA3001.

179. Parekh P, Joos F, Müller SA. A modeling assessment of the interplay between aeolian iron fluxes and iron-binding ligands in controlling carbon dioxide fluctuations during Antarctic warm events. Paleoceanography. 2008;23(4):PA4202.

180. Tagliabue A, Bopp L, Roche DM, Bouttes N, Dutay J-C, Alkama R, et al. Quantifying the roles of ocean circulation and biogeochemistry in governing ocean carbon-13 and atmospheric carbon dioxide at the last glacial maximum. Clim Past. 2009;5(4):695–706.

181. Nickelsen L, Oschlies A. Enhanced sensitivity of oceanic CO_2 uptake to dust deposition by iron-light colimitation. Geophys Res Lett. 2015;42(2):492–9.

182. Muglia J, Somes CJ, Nickelsen L, Schmittner A. Combined effects of atmospheric and seafloor iron fluxes to the Glacial Ocean. Paleoceanography. 2017;32(11):1204–18.

183. Sigman DM, Hain MP, Haug GH. The polar ocean and glacial cycles in atmospheric CO2 concentration. Nature. 2010;466(7302):47–55.

184. Murray RW, Leinen M, Knowlton CW. Links between iron input and opal deposition in the Pleistocene equatorial Pacific Ocean. Nat Geosci. 2012;5(4):270–4.

185. Kienast SS, Hendy IL, Crusius J, Pedersen TF, Calvert SE. Export production in the subarctic North Pacific over the last 800 kyrs: no evidence for iron fertilization? J Oceanogr. 2004;60(1):189–203.

186. Tagliabue A, Aumont O, Bopp L. The impact of different external sources of iron on the global carbon cycle. Geophys Res Lett. 2014;41(3):920–6.

187. Saito MA, Noble AE, Tagliabue A, Goepfert TJ, Lamborg CH, Jenkins WJ. Slow-spreading submarine ridges in the South Atlantic as a significant oceanic iron source. Nat Geosci. 2013;6(9):775–9.

188. Hain MP, Sigman DM, Haug GH. Carbon dioxide effects of Antarctic stratification, North Atlantic intermediate water formation, and subantarctic nutrient drawdown during the last ice age: diagnosis and synthesis in a geochemical box model. Glob Biogeochem Cycles. 2010;24(4):GB4023.

189. Martínez García A, Winckler G. Iron fertilization in the glacial ocean. In: Dust. Pages, vol. 22: Past Global Changes Magazine; 2014. p. 82–3.

190. Baker AR, Croot PL. Atmospheric and marine controls on aerosol iron solubility in seawater. Mar Chem. 2010;120(1–4):4–13.

191. SCOR Working Group. GEOTRACES—an international study of the global marine biogeochemical cycles of trace elements and their isotopes. Chem Erde - Geochem. 2007;67(2):85–131.

192. Meskhidze N, Johnson MS, Hurley D, Dawson K. Influence of measurement uncertainties on fractional solubility of iron in mineral aerosols over the oceans. Aeolian Res. 2016;22:85–92.

193. Raiswell R, Hawkings JR, Benning LG, Albani S, Mahowald N. Comments on 'Influence of measurement uncertainties on fractional solubility of iron in mineral aerosols over the oceans' Aeolian Research 22, 85–92. Aeolian Res. 2017;25:123–5.

194. Shoenfelt EM, Sun J, Winckler G, Kaplan MR, Borunda AL, Farrell KR, et al. High particulate iron(II) content in glacially sourced dusts enhances productivity of a model diatom. Sci Adv. 2017;3(6):e1700314.

195. Journet E, Balkanski Y, Harrison SP. A new data set of soil mineralogy for dust-cycle modeling. Atmos Chem Phys. 2014;14(8): 3801–16.

196. Scanza RA, Mahowald N, Ghan S, Zender CS, Kok JF, Liu X, et al. Modeling dust as component minerals in the community atmosphere model: development of framework and impact on radiative forcing. Atmos Chem Phys. 2015;15(1):537–61.

197. Perlwitz JP, Pérez García-Pando C, Miller RL. Predicting the mineral composition of dust aerosols—part 2: model evaluation and identification of key processes with observations. Atmos Chem Phys. 2015;15(20):11629–52.

198. Lambert F, Bigler M, Steffensen JP, Hutterli M, Fischer H. Centennial mineral dust variability in high-resolution ice core data from Dome C, Antarctica. Clim Past. 2012;8(2):609–23.